中国低活马氏体钢熔化焊接头硬度与微观组织

雷玉成[1], 顾康家[1], 朱 强[1], 陈希章[1], 巨 新[2], 常凤华[3]

(1. 江苏大学 材料科学与工程学院, 江苏 镇江 212013;
2. 北京科技大学 物理系, 北京 100083; 3. 哈尔滨焊接技术培训中心, 哈尔滨 150046)

雷玉成

摘 要: 针对 4 mm 厚的中国低活马氏体钢, 采用 TIG 焊接方法分别对预热和未预热两组试样进行了焊接和焊后回火处理, 对焊接接头的硬度和微观组织结构进行了测试和观察. 结果表明, 焊缝区硬度值偏高, 靠近母材的热影响区出现较窄的软化带; 焊接接头金相组织为板条特征明显的回火马氏体组织, 未预热试样的马氏体含量与预热试样相比较, 两者之间没有明显的差异. 在晶内和晶界处分布大量的碳化物, 焊缝区为尺寸较小的棒状, 母材和热影响区为尺寸较大的颗粒状, 接头的组织和碳化物的析出对焊接接头的硬度有很大的影响.

关键词: 中国低活马氏体钢; 硬度; 马氏体; 碳化物

中图分类号: TG115.28 文献标识码: A 文章编号: 0253-360X(2009)11-0009-04

0 序 言

核聚变研究的长期目标是利用核聚变能满足人类的未来能源需求[1], 建造和运行国际热核聚变实验堆(international thermonuclear experimental reactor, ITER)是确定核聚变能能否有效地被人类用于大规模能源生产的必要步骤[1,2]. 由于低活化铁素体/马氏体钢(reduced activation ferritic/martensitic, RAFM)具有较低的辐照肿胀和线膨胀系数、较高的热导率等优良的热物理性能和力学性能, 以及相对较为成熟的技术基础, 因此被普遍认为是未来聚变示范堆和聚变动力堆的首选结构材料[2]. 目前世界各国均在发展和研究各自的 RAFM 钢, 如日本的 F82H 和 JLF-1, 欧洲的 EUROFER97 以及美国的 9Cr2WVTa 等[1-3].

中国低活马氏体钢(China low activation martensitic, CLAM)是具有中国自主知识产权的、成分及性能优化的 RAFM 钢[4]. CLAM 钢被定为中国设计研究的 ITER 试验包层模块的首选结构材料. 由于低活化的要求, CLAM 钢和其它低活化钢一样, 采用 W, Ta 和 V 等合金元素来取代常规铁素体/马氏体钢中的 Mo, Nb 和 Ni 等元素. 目前, CLAM 钢的物理性能、力学性能、微观组织结构及热等静压焊等已得到初步研究[4-6].

焊接技术是核聚变堆工程制造中不可缺少的关键技术, 同时, 焊接技术和工艺是 CLAM 钢走向实际应用的关键技术之一. 文中针对薄板 CLAM 钢, 采用 TIG 焊接方法对焊前预热和未预热两种试样进行了焊接和焊后回火处理, 对焊接接头质量进行了无损检测, 对焊接接头的硬度和微观组织结构进行了观测和分析.

1 试验方法

试验材料采用经过热处理的 12 mm 厚 CLAM 钢板材, 热处理工艺为 980 ℃/30 min 水冷淬火, 然后 760 ℃/90 min 回火处理, 化学成分见表 1. 其微观组织为板条马氏体, 并在晶内和晶界处分布着尺寸大约为 30 ~ 100 nm 起到弥散强化作用的析出碳化物, 主要为 $M_{23}C_6$ 型碳化物[1,2].

12 mm 厚的板材经线切割加工成厚度为 4 mm 的薄板, 坡口为 60° V 形坡口, 对试样进行双层对接焊, 第一层为打底层, 第二层为盖面层, 如图 1 所示. 填充焊丝直径为 2 mm, 从 CLAM 钢母材上切取. 试样分为两组, 其中对 1 号试样进行了焊前预热(150 ℃/20 min)和层间温度控制(180 ℃), 目的是为了防止焊接冷裂纹的产生, 降低焊缝冷却速度, 期望获得良好的组织和综合性能; 2 号试样则未进行焊前预热.

收稿日期: 2008-09-29
基金项目: 国家 973 计划基金资助项目(2008CB717802); 江苏大学科技创新团队资助项目(JD000019)

表 1 CLAM 钢的化学成分(质量分数, %)

Table 1 Chemical compositions of CLAM

Cr	W	V	Ta	Mn	C	S	Si	O	N	Co	Cu	Al	Ti	Ni	Fe
8.910	1.440	0.200	0.150	0.350	0.120	0.003	0.066	0.002	0.008	0.006	0.028	0.180	0.004	0.043	余量

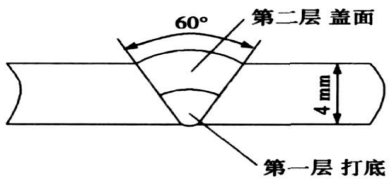

图 1 焊接示意图

Fig. 1 Welding schematic

焊接完成后, 为消除焊缝内应力和获得稳定的组织和性能, 两组试样都进行了 760 ℃/30 min 焊后回火热处理. 对热处理后的焊接接头进行了 X 射线无损检测, 检测结果未发现冷裂纹等焊接缺陷, 评定为 I 级焊缝. 随后截取了焊接接头的横截面, 利用维氏显微硬度计、金相显微镜(LEICA DM 2500M 正置透反射显微镜)和扫描电镜(SEM, JEOL — JSM — 7001F)对接头的硬度和微观组织结构进行了测试和观察.

2 试验结果与分析

2.1 组织结构

经过焊后回火处理后的焊接接头金相组织如图 2 所示. 焊缝、热影响区和母材都显示为板条特征明显的回火马氏体组织, 焊缝区晶粒明显粗大. 虽然 1 号试样进行了焊前预热, 冷却速度较未预热的 2 号试样慢, 但两者间焊缝区晶粒尺寸并无明显差别, 而且焊缝中马氏体含量也未见明显差异. 在焊接过程中, 熔池内液态金属同钢锭一样, 经历了晶核生成和晶核长大的过程, 熔池内液态金属由于电弧的加热, 处于过热状态, 平均温度可达到 1 770 ℃ ±100 ℃, 但熔池体积小, 周围有冷金属, 中心和边缘有较大的温度梯度, 加之熔敷金属没有控轧和形变热处理的机会, 焊缝组织不能细化, 因此焊缝区得到粗大的马氏体组织; 而靠近焊缝的热影响区(过热区), 由于受焊接热循环影响, 金属处于过热状态(固相线以下到 1 100 ℃左右), 焊接温度场分布极不均匀, 致使焊缝附近的过热区奥氏体晶粒急剧长大, 且温度越高奥氏体晶粒长大速度越快, 因此也形成粗大的奥氏体晶粒, 在马氏体转变相区内, 奥氏体转变为完全板条马氏体, 导致焊缝附近的热影响区(过热区)中最终也形成粗大的板条马氏体组织. 在试样经过焊后回火处理后, 得到性能优于板条马氏体的回火马氏体组织.

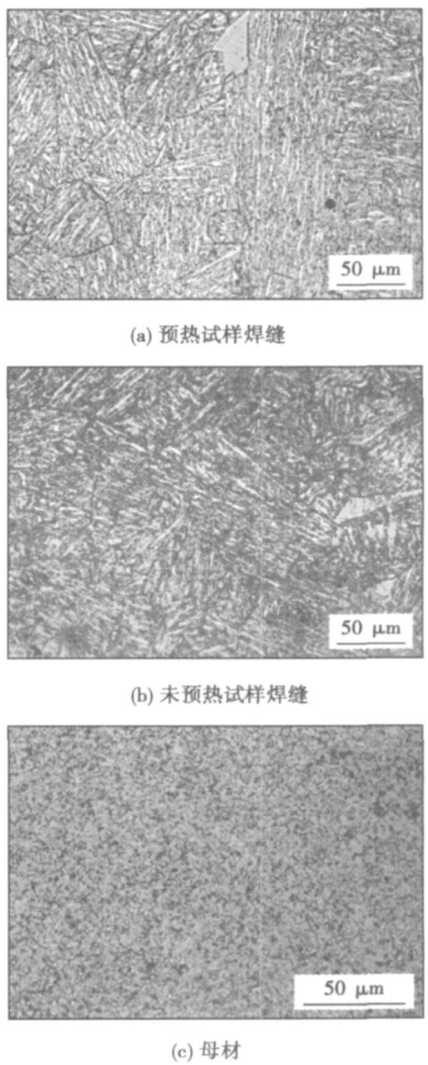

图 2 焊缝和母材金相组织形貌

Fig. 2 Optical micrograph of weld metal and base metal

图 3 为焊接接头各区域中碳化物分布情况, 由图 3 可以看出, 在原奥氏体晶界和晶内析出了大量碳化物, 它们大部分分布在晶界和马氏体板条界上, 根据文献[2]可知析出的碳化物主要是 $M_{23}C_6$, 在焊缝区, 碳化物的尺寸较小, 多为棒状, 长度在 50 ~ 200 nm 之间; 熔合线附近碳化物形状和焊缝区相似, 但尺寸略大; 热影响区(回火区)和母材内的碳化

物多为颗粒状，直径在 100～500 nm 之间.

低碳钢的板条马氏体形成温度高，发生自回火现象，在其形成后过饱和的碳发生部分分解，在马氏体晶体内析出碳化物质点，并导致形成立方马氏体.

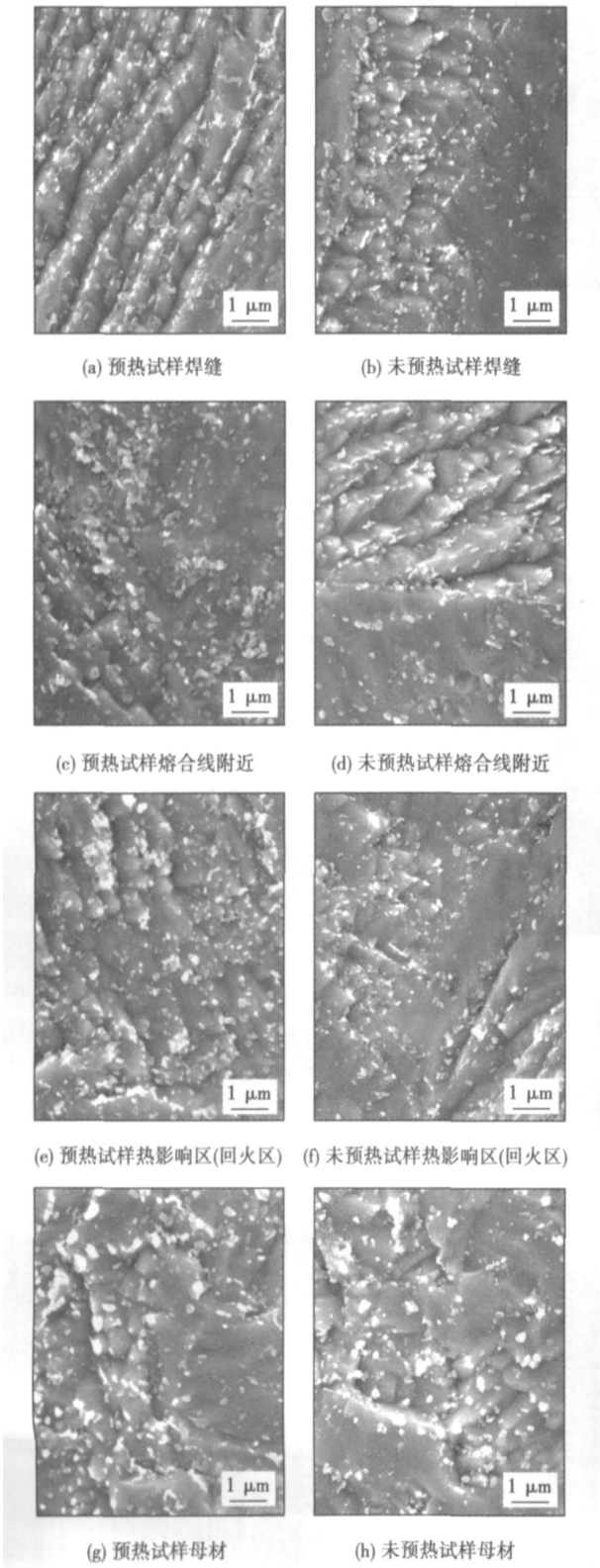

图 3　碳化物分布图

Fig. 3　Carbide distributions

碳化物的转变主要取决于回火温度，由于焊后进行了 760 ℃高温回火处理，马氏体发生分解，已脱离共格关系的渗碳体开始明显地聚集长大，出现球化和粗化现象，因此热影响区（回火区）和母材均出现了较大的颗粒状碳化物.

2.2　硬度测试与分析

硬度测试使用了维氏显微硬度计对焊接接头的横截面进行了测试，试验力为 100 N，测得了焊缝、热影响区和母材区的维氏硬度，并对 1 号预热试样分别测试了接头盖面层和打底层的硬度. 经过焊后热处理的 1 号试样和 2 号试样的接头横截面分别如图 4a，c 所示，在这些横截面上测试的硬度值分别如图 4b，d 所示. 结果显示，经过 150 ℃预热的 1 号试

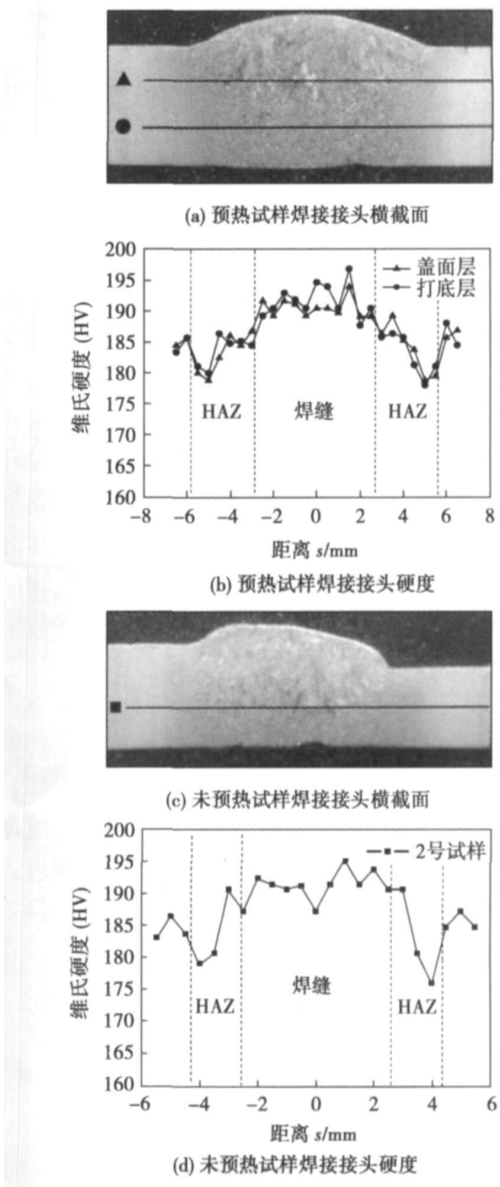

图 4　接头横截面和显微硬度

Fig. 4　Cross-sections and hardness distributions

样盖面层平均硬度为 190.6 HV，高于母材的平均硬度 185.7 HV，而打底层的平均硬度为 191.8 HV 同盖面层的平均硬度(190.6 HV)基本相同. 两组试样都在接近母材的热影响区出现了大约 1 mm 宽的软化区. 2 号试样焊缝区硬度为 191.6 HV，同 1 号试样焊缝区硬度基本相同，说明焊前预热对薄板 CLAM 钢熔化焊接头的硬度影响不大. 两组试样均出现了焊缝区硬度高于母材和热影响区的现象，但两组试样都没有出现非常明显的硬化现象.

从接头各区域的组织结构和碳化物的析出形状大小及分布可以解释几个区域的硬度变化. 马氏体高强度、高硬度的原因是多方面的，其中主要包括碳原子的固溶强化、相变强化以及时效强化，对于板条马氏体的硬度主要取决于其含碳量，随含碳量的增加而增加，合金元素的增加对马氏体的硬度影响不大[7].

在焊接接头中，焊缝区和附近热影响区(过热区)得到硬度偏高的粗大板条马氏体组织. 虽然经过高温回火后得到回火马氏体，但硬度仍然高于母材. 因为焊缝区马氏体分解过程中析出的碳化物颗粒小弥散强化作用强，而母材内的碳化物颗粒大，弥散强化作用弱，从而导致焊缝区硬度高于母材. 但是焊缝区没有出现明显的硬化现象是因为经过高温回火后，碳化物得到充分析出，晶格畸变减少，从而降低了组织的脆性.

靠近母材的热影响区(回火区)，受焊接热循环的影响，经历加热(温度低于 A_1)冷却的过程，相当于又经历一次回火过程. 在此过程中会有马氏体的分解及碳化物的聚集长大，弥散强化作用减弱，但晶粒尺寸并无明显变化，因此硬度下降，出现一条较窄的软化区.

3 结 论

(1) 焊前预热与未预热两组试样，均为 I 级焊缝，未发现焊接缺陷，两者之间的组织结构和硬度皆无明显差别，说明焊前预热对薄板 CLAM 钢的焊接影响不明显.

(2) 焊后回火处理后的接头金相组织为板条特征明显的回火马氏体，焊缝区和熔合线内碳化物为棒状，分布在原奥氏体晶界和马氏体板条上，粗大的马氏体组织导致焊缝区和过热区硬度略高于母材，但焊缝未出现明显硬化现象.

(3) 靠近母材的热影响区(回火区)有马氏体的分解及碳化物的聚集长大，弥散强化作用减弱，因此硬度下降，出现一条较窄的软化区.

参考文献:

[1] Hong B G, Lee D W, Wang S J, *et al*. Basic concepts of DEMO and a design of a helium-cooled molten lithium blanket for a testing in ITER[J]. Fusion Engineering and Design, 2007, 82(15－24): 2399－2405.

[2] Klueh R L, Gelles D S, Jitsukawa S, *et al*. Ferritic/martensitic steels overview of recent results[J]. Journal of Nuclear Materials, 2002, 307－312(1): 455－465.

[3] Salavy J F, Boccaccini L V, Lässer R, *et al*. Overview of the last progresses for the European test blanket modules projects[J]. Fusion Engineering and Design, 2007, 82(15－24): 2105－2112.

[4] 黄群英, 李春京, 李艳芬, 等. 中国低活化马氏体钢 CIAM 研究进展[J]. 核科学与工程, 2007, 27(1): 41－50.
Huang Qunying, Li Chunjing, Li Yanfen, *et al*. R&D status of China low activation martensitic steel[J]. Chinese Journal of Nuclear Science and Engineering, 2007, 27(1): 41－50.

[5] 刘松林, 汪卫华, 龙鹏程, 等. 聚变发电反应堆双冷液态锂铅包层模块结构设计与分析[J]. 核科学与工程, 2005, 25(1): 91－96.
Liu Songlin, Wang Weihua, Long Pengcheng, *et al*. Structural design and analysis of dual-cooled lithium-lead blanket module for the fusion power reactor FDS－Ⅱ[J]. Chinese Journal of Nuclear Science and Engineering, 2005, 25(1): 91－96.

[6] Huang Q, Li C, Li Y, *et al*. Progress in development of China low activation martensitic steel for fusion application[J]. Journal of Nuclear Materials, 2007, 367－370(1): 142－146.

[7] 崔忠圻. 金属学与热处理[M]. 北京: 机械工业出版社, 2000.

作者简介: 雷玉成, 男, 1962 年出生, 教授, 博士生导师. 主要从事焊接工艺及设备、焊接过程控制及模拟、先进连接技术等方面的研究与开发. 发表论文 80 余篇.

Email: yclei@ujs.edu.cn

MAIN TOPICS, ABSTRACTS & KEY WORDS

Tele-operated TIG welding robot for hyperbaric underwater pipeline repair welding JIAO Xiangdong[1], ZHOU Canfeng[1], XUE Long[1], GAO Hui[1], FANG Xiaoming[2] (1. Research Center of Joining Technology in Ocean Engineering, Beijing Institute of Petrochemical Technology, Beijing 102617, China; 2. China Offshore Oil Engineering Co. LTD., Tianjin 300452, China). p 1—4

Abstract: Among the available underwater pipeline repair methods, hyperbaric TIG welding technology may be the easier one to obtain better joint quality. Due to the low automation level and the bevel preparation difficulty, the repair welding should be conducted based on both the welding knowledge of the welder on deck and the operation skill of the diver. A tele-operated robot for all position hyperbaric pipe welding was developed. In the specified case of underwater welding, the process was controlled by a surface based operator, a clear and real time image of the arc as well as the image of groove location were required. An observation system of three cameras for chamber, groove and weld was also developed respectively. All the necessary message of vision, welding current and arc voltage were collected and transferred to the surface by the developed computerized information system. The underwater pipeline maintanence system consists of the welding robot, observation system, the information system, together with the habitation. The chamber gas type, the welding power source and arc striking were also studied. With the welding proceedure developed in the hyperbaric welding laboratory, a good weld was obtained in a underwater pipe repair welding test at Bohai sea.

Key words: tele-operated robot; underwater welding; underwater pipeline repairing; welding robot

Electron beam welding of TC21 titanium alloy with large thickness ZHANG Binggang[1], WANG Ting[1], CHEN Guoqing[1], LIU Chenglai[2], LIU Yulong[1] (1. State Key Laboratory of Advanced Welding Production Technology, Harbin Institute of Technology, Harbin 150001, China; 2. Shenyang Liming Aero-Engine (Group) Co. LTD., Shenyang 110000, China). p 5—8

Abstract: Electron beam welding of TC21 56 mm titanium alloy was carried out. The microstructure and the mechanical properties of welded joints were analyzed and tested. The results showed that the weld zone consisted of the columnar β grains, and in which the transgranular acicular α′ martensite were dispersedly distributed. HAZ can be divided into three parts from base metal to weld zone, which are the equiaxed recrystallized β grain zone, Widmanstaten structure zone formed by lamellar and acicular α phases and lamellar α phase coarsening zone. Fusion zone consists of the adnate columnar and equiaxed grains. Tensile strength of joints reaches to that of base metal and the failure appears in the base metal. The mechanical properties are uniform along the vertical direction. Plasticity in the welded joint is greatly decreased and only up to 50% of that of the base metal. The microhardness in weld zone is the highest, and that of the equiaxed grain zone and Widmanstaten structure zone in HAZ is higher, and the microhardness in columnar α phase coarsening zone is the lowest.

Key words: TC21 titanium alloy; electron beam welding; microstructure; mechanical properties

Hardness and microstructure of China low activation martensitic steel fusion welded joint LEI Yucheng[1], GU Kangjia[1], ZHU Qiang[1], CHEN Xizhang[1], JU Xin[2], CHANG Fenghua[3] (1. School of Materials Science and Engineering, Jiangsu University, Zhenjiang 212013, Jiangsu, China; 2. Physics Department, University of Science and Technology of Beijing, Beijing 100083, China; 3. Harbin Welding Training Institute, Harbin 150046, China). p 9—12

Abstract: The preheated and non-preheated 4 mm China low activation martensitic steel (CLAM) plate were welded by TIG welding and post-weld heat treating, and the hardness and microstructure in welded joint were tested and observed. The results show that the hardness in the weld metal is higher and the softening band appears in the heat-affected zone (HAZ) closing to the base metal. The tempered lath martensite is observed in welded joints. There is no significant difference in martensite content between the preheated and non preheated weldments. A large amount of carbide particles are observed in the grains and at the grain boundary. The carbides are small rods in weld metal and large granular in the HAZ and base metal respectively. The microstructure and carbides in welded joints have great effect on the hardness.

Key words: China low activation martensitic steel; hardness; martensite; carbide

Numerical analysis on stress distribution in adhesive-welded double lap joint of aluminum YOU Min[1], LI Zhi[1,2], ZHAO Meirong[1], GUO Bin[2], YAN Jialing[1] (1. Hubei Key Laboratory of Hydroelectric Machinery Design & Maintenance, China Three Gorges University, Yichang 443002, Hubei, China; 2. Mechanical and Electric Engineering Department, China Three Gorges Project Corporation, Yichang 443002, Hubei, China). p 13—16

Abstract: The influence of the elastic modulus of adhesives and nuggets position on the stress distribution in adhesive-welded double lap joints of aluminum was investigated by elastic-plastic finite element method (FEM). The results obtained show that the influence of the elastic modulus of adhesive on the stress distribution in adhesive-welded double lap joints of aluminum is significant. The load subjected by the nuggets is greater when the elastic modulus of adhesive is lower and the load subjected by the adhesive layer increases when the elastic modulus of adhesive is higher. The effect of nuggets location is also significant when the center of the nugget is moved to the left end of the overlap zone. The peak stress along the mid-bonding line of the aluminum double lap joint increases when the center of the nuggets are moved to near the left end of the overlap zone. The peak value of the von mises equivalent stress increases from 55.2 MPa to 77.4 MPa when the nugget center is shifted from the point at 12.5 mm to 5.5 mm. Therefore, the load bearing ability of the adhesive-welded double lap joints of aluminum can be im-